Clinical Chemistry 45:5
638–650 (1999)

Enzymes and Protein Markers

Anti-Free Prostate-specific Antigen Monoclonal Antibody Epitopes Defined by Mimotopes and Molecular Modeling

Sandrine Michel,[1] Gilbert Deléage,[2] Jean-Philippe Charrier,[1] Jacques Passagot,[1] Nicole Battail-Poirot,[1] Geneviève Sibai,[1] Michel Jolivet,[1] and Colette Jolivet-Reynaud[3*]

Background: **Prostate-specific antigen (PSA) is an important marker for the diagnosis and management of prostate cancer, and the free PSA/total PSA ratio has been shown to be efficient for distinguishing prostate cancer from benign prostatic hyperplasia. We report here the characterization of seven mouse monoclonal antibodies (mAbs) and the partial localization of two conformational epitopes identified by anti-free PSA mAbs.**

Methods: **The mAbs were studied by competition and sandwich assays, and the epitope localization of the two anti-free PSA mAbs (6C8D8 and 5D3D11) was performed using phage displayed peptide libraries and molecular modeling.**

Results: **The seven mAbs were classified into three groups according to their recognition specificities and their ability to inhibit the enzymatic activity of PSA and the formation of PSA-α_1-antichymotrypsin (ACT) complex. Among the anti-free PSA mAb group, 6C8D8 recognized the phage displayed peptide RKLRPHWLHFHPVAV, two parts of which presented similarities with two regions distant on the PSA sequence but joined in the tridimensional structure. mAb 5D3D11 recognized the peptide DTPYPWGWLLDEGYD, which is similar to a PSA region located on the board of the groove containing the PSA enzymatic site. Both epitopes were located in the theoretical ACT binding site described previously. Moreover, these mAbs were able to inhibit the enzymatic activity of PSA.**

Conclusions: **These epitope localizations are in agreement with the ability of both mAbs to inhibit enzymatic activity and ACT fixation. The results presented here could bring information for the generation of clinically relevant PSA assays.**

Prostate-specific antigen (PSA),[4] a 237-amino acid glycoprotein (33 kDa) that belongs to the kallikrein serine protease family *(1)*, is produced in the secretory epithelium of the prostate gland. PSA, also called human glandular kallikrein 3 *(2)*, is released physiologically from the prostate into seminal fluid at concentrations of 0.2–5 g/L *(3)*, whereas in the serum of healthy males, PSA was found in concentrations lower than 2.5 μg/L *(4)*. During prostate cancer, PSA enters into the circulation, leading to increased PSA concentrations in the blood *(5)*. Therefore, the measurement of serum PSA appears to be an important marker for the diagnosis and management of prostate cancer. PSA increases in serum can also be seen in patients with bacterial prostatitis or benign prostatic hyperplasia (BPH).

PSA exists in serum in different molecular forms that can be measured separately and contribute to discrimination between BPH and prostate cancer. In serum, PSA forms stable complexes with several extracellular protease

[1] bioMérieux, Département R&D unité Immunoessais, Chemin de l'Orme, 69280 Marcy L'Etoile, France.
[2] Institut de Biologie et de Chimie des Proteines, Unite Propre de Recherche, 412/Centre National de la Recherche Scientifique, 7 passage du Vercors, 69367 Lyon Cedex 07, France.
[3] Unite Mixte de Recherche, 103 bioMérieux/Centre National de la Recherche Scientifique, ENS, 46 allée d'Italie, 69364 Lyon Cedex 07, France.
* Address correspondence to this author at: UMR 103 bioMérieux/CNRS, ENS, 46 allée d'Italie, 69364 Lyon Cedex 07, France. Fax 33-4-72 72 85 33; e-mail colette.jolivet@ens-bma.cnrs.fr.
Received December 23, 1998; accepted February 25, 1999.

[4] Nonstandard abbreviations: PSA, prostate-specific antigen; BPH, benign prostatic hyperplasia; ACT, α_1-antichymotrypsin; A2M, α_2-macroglobulin; f-PSA, free PSA; t-PSA, total PSA; mAb, monoclonal antibody; PBS, phosphate-buffered saline; PBS-T, PBS-Tween 20; BSA, bovine serum albumin; TBS, Tris-buffered saline; and TBS-T, TBS-Tween 20.

inhibitors, predominantly α_1-antichymotrypsin (ACT) and α_2-macroglobulin (A2M), referred as serpins. This causes the inactivation of the chymotrypsin-like activity of PSA *(6)*. PSA-ACT is the predominant immunoreactive form in serum and can be detected in substantial amounts *(7)*. The conditions commonly used in laboratory and commercial immunoassays do not permit the detection of PSA-A2M because PSA is completely encompassed in the 720-kDa A2M molecule. However, the PSA-A2M complex can be measured by the use of immunological methods as described by Espana et al. *(8)*. Nevertheless, although the concentrations of A2M and ACT in the blood are sufficient to complex most of the PSA, there is a small immunoreactive fraction that represents free PSA (f-PSA). f-PSA may be an altered form that has lost its ability to bind serum inhibitors *(9)*.

Several studies have shown that the ratio of f-PSA to total PSA (t-PSA; i.e., free + ACT-bound PSA) is lower in prostate cancer patients than in BPH patients *(9, 10)*. Furthermore, clinical studies have confirmed the efficiency of using this ratio to distinguish prostate cancer from BPH patients, particularly in the diagnostic gray zone of 4–10 μg/L, where PSA concentrations overlap for cancer and non-cancer diseases *(11–14)*. However, one of the major problems is related to the specificity of the anti-PSA antibodies used in the current PSA commercial reagents *(15)*. These antibodies should not cross-react with anti-hK2 antibodies, directed against human kallikrein 2, a protein homologous to PSA *(16)*. Moreover, antibodies specific for t-PSA should recognize f-PSA as well as ACT-bound PSA on an equimolar basis.

To develop immunoassays for a differential diagnosis between prostate cancer and BPH, we raised anti-PSA mouse monoclonal antibodies (mAbs) and mapped their epitopes. We report here the characterization of three anti-f-PSA and four anti-t-PSA mAbs that facilitate the localization of antigenic determinants on the PSA molecule that discriminate either f-PSA or PSA-ACT and thus aid the selection of specific mAbs. We studied two nonoverlapping epitopes specifically recognized by two anti-f-PSA mAbs, using phage displayed peptide library technology. We used molecular modeling to localize these epitopes on the tridimensional representation of the PSA molecule, described previously by Villoutreix et al. *(17)*.

Materials and Methods

BIOLOGICAL MATERIAL

The PSA used in this study was of seminal origin and was supplied by Scipac. ACT and PSA-ACT complex were obtained from Scripps Laboratories.

mAbs

BALB/c JYco female mice, ages 4–6 weeks (IFFA Credo) were immunized by intraperitoneal injection with 15 μg of purified PSA emulsified with an equal volume of Freund's complete adjuvant, followed by five injections with incomplete adjuvant every 2 weeks. Four days after the last injection, spleen cells were harvested and fused according to Köhler and Milstein *(18, 19)* with the Sp 2/0-Ag14 mouse myeloma cell line. After the cells were grown for 12–14 days, the culture supernatants were screened with an ELISA in which the solid phase was coated with the antigen used for immunization. Positive colonies were subcloned twice by limiting dilution. Ascitic fluids were obtained from mice primed with a 0.5-mL intraperitoneal injection of Pristane and then injected with 10^6 hybridoma cells. IgG antibodies were purified on a Protein A-Sepharose 4FF column, according to the instructions of the manufacturer (Pharmacia).

BIOTINYLATION OF mAbs

Purified mAbs were biotinylated using sulfo-NHS-LC-biotin (Merck), according to the method of Gretch et al. *(20)*.

ELISA CHARACTERIZATION OF ANTI-PSA mAbs

Nunc 96-well plates (Nunc) were coated with 100 μL of 1 mg/L PSA or PSA-ACT complex in 0.05 mol/L carbonate buffer, pH 9.6. After incubation overnight at room temperature, the plates were washed three times with phosphate-buffered saline (PBS; 50 mmol/L phosphate buffer, pH 7.2, 150 mmol/L NaCl) containing 0.5 mL/L Tween 20 (PBS-T), and blocked for 1 h at 37 °C with PBS containing 10 g/L lyophilized milk extract. After the plates were washed a second time with PBS-T, 100 μL of ascitic fluid supernatant diluted 1:10 to $1:10^6$ in PBS-T was added and incubated for 1 h at 37 °C. The plates were washed with PBS-T, and 100 μL of alkaline phosphatase-conjugated goat anti-mouse IgG (Jackson ImmunoResearch Laboratories) was added at a 1:2000 dilution in PBS-T containing 10 g/L bovine serum albumin (BSA; Sigma). The plates were incubated for 1 h at 37 °C and then washed again with PBS-T. The substrate, a solution of *p*-nitrophenylphosphate (Sigma), was added for 30 min. Enzymatic activity was blocked with 1 mol/L NaOH, and the absorbance was measured at 405 nm with an ELISA plate reader (bioMérieux).

EQUIMOLARITY OF RECOGNITION OF f-PSA AND PSA-ACT

The equimolarity of f-PSA and PSA-ACT recognition was determined in a sandwich assay by use of the mAb to be studied and a goat anti-PSA polyclonal antibody. ELISA plates were coated with 100 μL of goat anti-mouse IgG (Jackson ImmunoResearch) at a 1:2000 dilution in 0.05 mol/L carbonate buffer, pH 9.6. After incubation overnight at room temperature, the plates were washed three times with PBS-T and blocked for 1 h at 37 °C as described above. The plates were washed with PBS-T, and 100 μL of ascitic fluid supernatant diluted 1:10 to $1:10^6$ in PBS-T was added and incubated for 1 h at 37 °C. After the plates were washed with PBS-T, 100-μL aliquots of mixtures containing different ratios of PSA and PSA-ACT (10:90, 50:50, or 90:10) at a final PSA concentration of 1 mg/L

were added and incubated for 1 h at 37 °C. The plates were washed and then incubated with an alkaline phosphatase-conjugated goat anti-PSA polyclonal antibody (Scantibodies Laboratories) at a 1:200 dilution in PBS-T containing 10 g/L BSA for 1 h at 37 °C. The plates were then washed, developed, and read as described above. The mAb recognition was considered equimolar if the assay gave the same molar response for f-PSA and PSA-ACT.

sodium dodecyl sulfate-polyacrylamide gel electrophoresis and western blotting

PSA and PSA-ACT were separated on 12% sodium dodecyl sulfate-polyacrylamide gels as described by Laemmli *(21)*. Samples were denatured before electrophoresis nonreducing conditions (with Laemmli buffer) or under reducing conditions (with Laemmli buffer containing 140 mmol/L β-mercaptoethanol). After separation, the proteins were transferred to polyvinylidene fluoride membranes (Millipore), according to the method of Towbin et al. *(22)*, and blocked with 50 g/L nonfat milk in Tris-buffered saline (TBS; 20 mmol/ L Tris, pH 7.5, 500 mmol/L NaCl) for 2 h at room temperature. Anti-PSA mAbs diluted to a final concentration of 10 mg/L in TBS-milk containing 0.5 mL/L Tween 20 (TBS-T-milk) were incubated with the membranes overnight at 4 °C. The membranes were then washed three times with TBS-T and incubated with alkaline phosphatase-conjugated goat anti-mouse IgG (Jackson ImmunoResearch) at a 1:5000 dilution in TBS-T-milk (1 h, room temperature). After the membranes were washed twice with TBS-T and once with borate buffer (31.5 mmol/L borate, pH 9.7, 10 mmol/L $MgSO_4$), the staining was developed by incubating the membranes 2 min with substrate solution (0.5 g/L β-naphthyl acid phosphate and 0.5 g/L tetrazotized *o*-dianisidine in borate buffer). The membranes were then rinsed with distilled water and dried at 37 °C.

evaluation of kinetic constants of mAbs

The binding of mAbs to PSA was measured by BIAcore analysis with the Fab′ forms of the mAbs to avoid the experimental and computational problems associated with the use of bidendate ligands, which has been described previously *(23, 24)*. All experiments were performed on a BIAcore 1000 instrument (Pharmacia Biosensor), according to the manufacturer's instructions. PSA was immobilized via the primary amine groups as described previously *(25)*, using *N*-hydroxysuccinimide/*N*-ethyl-*N*′(3-diethylaminopropyl)carbodiimide coupling reagents, to a final resonance value of 294 resonance units. HEPES-buffered saline [10 mmol/L HEPES, pH 7.4, 150 mmol/L NaCl, 3.4 mmol/L EDTA, 0.05 mL/L P20 (Pharmacia)] was used as the running buffer at a flow rate of 5 μL/min. Each Fab′ form of a mAb was diluted to 0.7–435 nmol/L in buffer. After injection, the flow of the running buffer was established to allow observation of the dissociation of bound PSA. The association and dissociation rates of each mAb were determined using BIAevaluation, Ver. 2.1 (Pharmacia Biosensor), according to methods described previously *(26)*. The affinity was calculated as follows: K_a = association rate (k_a)/dissociation rate (k_d), and expressed in L/mol.

competitive elisa for mAbs

ELISA plates were coated with 100 μL of 2 mg/L PSA in 0.1 mol/L carbonate buffer, pH 8.3. After incubation for 2 h at 37 °C, the plates were washed four times with PBS-T and blocked for 2 h at 37 °C with PBS containing 100 mL/L goat serum (PBS-goat serum). The plates were washed with PBS-T, and 100 μL of the first native anti-PSA mAb at a concentration of 50 mg/L in PBS-T-goat serum was added and incubated for 2 h at 37 °C. After the plates were again washed with PBS-T, 100 μL of the second biotinylated anti-PSA mAb diluted to 2–100 μg/L in PBS-T-goat serum was added and incubated for 2 h at 37 °C. The plates were washed with PBS-T, and 100 μL of peroxidase-conjugated streptavidin (Jackson ImmunoResearch) was added at a 1:5000 dilution in PBS-T-goat serum. The plates were incubated for 1 h at 37 °C and then washed with PBS-T. The plates were developed using a commercial color kit (bioMérieux) containing *o*-phenylenediamine and hydrogen peroxide. After a 10-min incubation, the reaction was stopped with H_2SO_4, and the plates were read at 492 nm with an ELISA plate reader. The values were expressed as the mean absorbance values of triplicate measurements.

sandwich assays

Sandwich assays experiments were performed using an automated quantitative enzyme-linked fluorescent assay developed on the VIDAS analyzer (bioMérieux) *(27, 28)*. The two-step capture/tag test relies on two mAbs, the second one being labeled with alkaline phosphatase as described previously *(29)*.

phage pentadecapeptide libraries

Two filamentous pentadecapeptide phage libraries were kindly provided by Prof. George Smith, Division of Biological Sciences, University of Missouri, Columbia, MO *(30)*. The libraries were constructed as follows.

The 15merVIII library was constructed in vector f88–4. A 330-bp noncoding region of fd-tet was replaced with a synthetic version of the major coat protein gene VIII. Thus, 15merVIII had two VIII genes in the same genome, of which one was wild-type and the other the foreign 15-mer residues. The numbers of primary clones and transductant clones amplified were 2×10^9 and 2.2×10^{12}, respectively. The concentration of phage particles was 1×10^{17} virions/L.

The 15merIII library was constructed in vector fUSE5. This vector differs from fd-tet in having two *Sfi*I sites along with a frameshift mutation engineered into gene III just downstream of the signal sequence. The library was constructed by splicing degenerate oligonucleotide inserts

into the *Sfi*I sites. The inserts restored the reading frame, leading to a recombinant gene-III protein (pIII) that was incorporated as a ring of five molecules at one tip of the virion. The numbers of primary clones and transductant clones amplified were 2×10^8 and 3.2×10^{11}, respectively. The concentration of phage particles was 1×10^{17} virions/L.

affinity purification of the phages

Biopannings of phages were performed according to published protocols *(30–32)* with some modifications. The screening of the two libraries was performed using the same protocol. Briefly, 10 μg of biotinylated anti-f-PSA IgG was coupled to 35-mm polystyrene Petri dishes (Falcon) coated with 10 μg of streptavidin. The dish was incubated overnight at 4 °C and washed six times with TBS-T. In the first round of biopanning, 10^{12} phages from the initial library were allowed to react with the dish-bound IgG for 4 h at 4 °C while the plate was rocking. The unbound phages were removed by repetitive washes with TBS-T. The bound phages were then eluted from the dish with 0.1 mol/L HCl, pH 2.2, containing 1 g/L BSA and 0.1 g/L phenol red and were amplified by infecting *Escherichia coli* K91 Kan cells, as described previously *(31)*. In the second, third, and fourth rounds of biopanning, 20% of the amplified phages from the preceding round were preincubated with 100, 10, and 1 nmol/L, respectively, of the biotinylated anti-f-PSA mAb overnight at 4 °C before being added to the 35-mm polystyrene Petri dish coated with 10 μg of streptavidin. The procedure was then identical to the first round.

clone selection

Phage eluates from the last round of biopanning were cloned as described previously *(30, 31)* and propagated in overnight cultures (1.7 mL) of infected K91 Kan cells. After the cells were removed, phages from the supernatants were precipitated twice with polyethylene glycol and then dissolved in 200 μL of TBS as reported previously *(30)*.

DNA sequencing

Single-stranded DNA was prepared from the purified phages as described by Sambrook et al. *(33)*. The nucleotide sequences of the gene VIII or gene III inserts were determined according to the modified method of Sanger et al. *(34)* with an Applied Biosystems DNA sequencer (Model 373A; Perkin-Elmer), using the Taq DyeDeoxy™ Terminator Cycle Sequencing Ready kit (Perkin-Elmer). Cycle sequencing was performed with either the primer 5′ HO-TGAAGAGAGTCAAAAGCAGC-OH 3′ or the primer 5′ HO-CCCTCATAGTTAGCGTAACG-OH 3′ corresponding, respectively, to either the wild-type phage f1 gene VIII sequence or the fUSE5 gene III sequence. The amino acid sequence was deduced from the nucleotide sequence.

ELISA using supernatant phages

The plates were coated with 100 μL of native anti-f-PSA mAb (used for screening the library) at a concentration of 10 mg/L in PBS by incubation for 2 h at 37 °C and washed four times with TBS-T. The plates were then blocked with TBS containing 10 g/L BSA for 2 h at 37 °C and washed with TBS-T, after which 100 μL of supernatant containing phages diluted in TBS was added to the wells. After the plates were incubated overnight at 4 °C, unbound phages were removed by four washes with TBS-T. Bound phages were detected in a sandwich assay with 100 μL of a biotinylated sheep antibody to M13 phage (5Prime → 3Prime) at a 1:5000 dilution in TBS-T-BSA for 2 h at 37 °C, and a peroxidase-conjugated streptavidin (Jackson ImmunoResearch) at a 1:5000 dilution in TBS-T-BSA for 1 h at 37 °C. The plates were developed and read as described above. The values were the mean absorbance values of triplicate measurements.

sequence analysis

The amino acid sequences of peptides and PSA were compared by use of the MacVector, Ver. 4.5 software (Kodak). Basically, the regions of highest similarity were detected with the LFASTA program, which tentatively searches for best local identities *(35)*. The PSA sequence was obtained from the literature *(36, 37)*. Some of the highest hits are indicated in Fig. 3.

molecular display

The tridimensional structure of PSA was obtained from the Protein Data Bank (PDB code, 1PFA.PDB). The visualization of the molecule was performed with the help of the RASMOL program *(38)*. The putative conformational epitopes were investigated on the basis of the proximity of their amino acids and on immunological data.

peptide synthesis

Peptide synthesis was carried out as described previously *(39)*. Biotinylation of peptides was selectively performed at the N-terminal end after deprotection of the last coupled amino acid fluorenyl methyloxycarbonyl group according to Deibel et al. *(40)*.

assays with synthetic peptides

ELISA plates were coated with 100 μL of 10 mg/L native 5D3D11 or 6C8D8 in PBS. After incubation overnight at 4 °C, the plates were washed four times with PBS-T and blocked for 2 h at 37 °C with PBS-goat serum. The plates were washed with PBS-T, and 100 μL of PSA diluted to 0.02–1 mg/L in PBS-T-goat serum was added and incubated 2 h at 37 °C. The plates were washed with PBS-T, and 100 μL of biotinylated peptide diluted to 10–100 mg/L in PBS-T-goat serum was added. The plates were washed with PBS-T, incubated with peroxidase-conjugated streptavidin, developed, and read as described above. The values were expressed as the mean absorbance values of triplicate measurements, and the standard de-

viation was calculated. The inhibition of peptide binding to its corresponding mAb by PSA was calculated as follows: 1 − (absorbance obtained in the presence of PSA/absorbance obtained in the absence of PSA), and expressed as a percentage.

DETERMINATION OF PSA ENZYMATIC ACTIVITY

The PSA enzymatic activity was determined by hydrolysis of the substrate MeO-Suc-Arg-Pro-Tyr-pNA · HCl (S-2586; Chromogenix AB) at the final concentration of 5 mmol/L in 50 mmol/L Tris-HCl, pH 7.8, 0.1 mol/L NaCl *(6)*. Hydrolysis was measured at 405 nm in an ultraviolet recording spectrophotometer (Beckman DU62). All reactions were performed at 37 °C and initiated by the addition of 5 μg of PSA. The absorbance was monitored for 30 min.

INHIBITION OF PSA-ACT COMPLEX FORMATION BY ANTI-f-PSA mAbs

ELISA plates were coated with 100 μL of 5 mg/L native anti-t-PSA mAb in PBS for 2 h of incubation at 37 °C and blocked with PBS-goat serum as described above. The plates were then washed four times with PBS-T, and 100 μL of 1 mg/L PSA in PBS-T-goat serum was added. After incubation overnight at 4 °C, the plates were washed four times with PBS-T, and 100 μL of 10 mg/L native anti-f-PSA mAb in PBS-T-goat serum was added and incubated for 15 min at 37 °C. After the plates were washed with PBS-T, 1 mg/L ACT in PBS-T-goat serum was added and incubated for 2 h at 37 °C. The plates were washed with PBS-T, and 100 μL of a 1:2000 dilution of rabbit anti-human ACT (Dako) in PBS-T-goat serum was added. After incubation for 2 h at 37 °C, the plates were washed with PBS-T, and 100 μL of a 1:5000 dilution of peroxidase-conjugated goat anti-rabbit IgG (Jackson ImmunoResearch) in PBS-T-goat serum was added. The plates were incubated for 1 h at 37 °C and then washed with PBS-T before being developed and read as described above. The values were expressed as the mean absorbance values of triplicate measurements. For each anti-t-PSA mAb-captured PSA, the complex formation in the absence of the second mAb corresponded to a relative 100% calibrator calculated as follows: mean absorbance obtained in the presence of ACT − mean absorbance obtained in the absence of ACT. This formula allowed the subtraction of the background attributable to the cross-reactivity between the anti-rabbit mAb and mouse mAbs. In the presence of a second mAb, the residual complex formation was determined using the same calculation and expressed as a percentage of the relative 100% calibrator. The assay was performed in the presence of goat serum as diluent. The possible presence of goat-serpin complexes that could interfere with the formation of the PSA-human ACT complex was ruled out by verification that the goat serum had no effect on the PSA proteolytic activity, determined as described above.

Results

CHARACTERIZATION OF ANTI-PSA mAbs

Seven anti-PSA mAbs were characterized for their specificity against the different forms of PSA. The affinity constants of the Fab′ forms of these mAbs against PSA, measured by the biosensor technology, ranged from 6×10^8 to 8×10^9 L/mol, except for 5D3D11, the affinity of which was $<10^7$ L/mol. As shown in Table 1, three mAbs bound only to f-PSA and thus could be considered as anti-f-PSA-specific, whereas four mAbs recognized both f-PSA and PSA-ACT. None of the tested mAbs were able to recognize ACT alone: the four anti-t-PSA mAbs that bound to PSA-ACT were specifically directed against PSA. However, when tested in sandwich assays with various ratios of PSA and PSA-ACT, only two of these mAbs (5D5A5 and 11E5C6) recognized PSA and PSA-ACT in equimolar amounts, whereas 5C10D9 and 7F2F2 bound more strongly to f-PSA than to PSA-ACT. Western blot experiments showed that under reducing conditions, PSA was not recognized by the three anti-f-PSA mAbs, indicating that the PSA three-dimensional structure maintained by five disulfide bridges was necessary for the antigen-mAb interaction. On the other hand, the four anti-t-PSA mAbs still recognized PSA under the same conditions. However, after limited proteolysis of PSA by

Table 1. Characterization of anti-PSA mAbs.

	ELISA recognition against[a]			Western blot recognition against[b]		
mAb	PSA	PSA-ACT	ACT	Reduced PSA	Nonreduced PSA	Affinity constant[c] against PSA, L/mol
6C8D8	++	−	−	−	+	6×10^8
5D3D11	++	−	−	−	+	$<10^7$
12E6H9	++	−	−	−	+	2×10^9
5C10D9	++	+	−	+	+	ND
7F2F2	++	+	−	+	+	1×10^9
5D5A5	++	++	−	+	+	8×10^9
11E5C6	++	++	−	+	+	2×10^9

[a] Specificity of anti-PSA mAbs was determined by ELISA as described in *Materials and Methods*. Equimolar recognition of f-PSA and PSA-ACT was determined in sandwich assays with various ratios of PSA and PSA-ACT as described in *Materials and Methods*.

[b] Immunoreactivity of anti-PSA mAbs against PSA under reduced or nonreduced conditions was determined by Western blot as described in *Materials and Methods*.

[c] Affinity constants of mAbs against PSA were determined by BIAcore analysis as described in *Materials and Methods*.

Table 2. Competition[a] of mAbs with themselves.

	Inhibition of binding of second mAb,[b] %						
	Second biotinylated mAb						
First mAb	6C8D8	5D3D11	12E6H9	5C10D9	7F2F2	5D5A5	11E5C6
6C8D8	68	5	62	12	20	0[c]	6
5D3D11	0[c]	68	0[c]	0[c]	0[c]	13	3
12E6H9	83	75	64	17	48	0[c]	0[c]
5C10D9	0[c]	0[c]	63	90	73	19	11
7F2F2	89	0[c]	84	51	78	0[c]	9
5D5A5	0[c]	0[c]	0[c]	96	0[c]	87	74
11E5C6	0[c]	0[c]	0[c]	0[c]	0[c]	32	87

[a] ELISA was performed as described in *Materials and Methods* with the seven mAbs described in Table 1.

[b] The inhibition percentage was calculated as follows: $\{1 - [(\text{absorbance}_{\text{mAb1+mAb2}} - \text{absorbance}_{\text{mAb1+control buffer}})/(\text{absorbance}_{\text{control buffer+mAb2}} - \text{absorbance}_{\text{mAb1+control buffer}})]\} \times 100$.

[c] For percentages less than 0%, the first mAb increased the fixation of the second.

trypsin, α-chymotrypsin, clostripain, or V8 protease, the resulting PSA proteolytic fragments were not immunoreactive as evidenced by Western blot analysis under reducing as well as nonreducing conditions (data not shown). Furthermore, as had also been observed by Piironen et al. *(41)* with their own mAbs, these mAbs were not able to recognize overlapping 9-mer peptides reproducing the linear PSA sequence (data not shown). Thus, these mAbs could also bind to a conformational epitope not destroyed when PSA was reduced in α-helix or β-layers.

complementarity of mAbs

According to competition experiments (Table 2) and sandwich assays (Table 3) using different mAb couples, 6C8D8, 5D3D11, and 12E6H9 did not inhibit the binding of 5D5A5 and 11E5C6. Thus, these different mAbs could represent two nonoverlapping groups of epitopes. Among the anti-f-PSA mAbs, the 6C8D8 and 12E6H9 epitopes appeared close to each other but different from the 5D3D11 epitope. Among the anti-t-PSA mAbs, 5D5A5 and 11E5C6 seemed to be similar but not identical. However, on the basis of their respective patterns of complementarity and competition, 5C10D9 and 7F2F2 were different from any of the other mAbs.

determination of 6c8d8 epitope by use of phage displayed peptide libraries

The mAb 6C8D8 (anti-f-PSA IgG) was used for screening the 15merIII phage library. After four rounds of biopanning, 72 clones of phages were isolated, their DNA was sequenced, and the motif amino acid sequences were deduced. As shown in Table 4, the isolated clones were separated into four groups. Group A contained the major selected motif (RKLRPHWLHFHPVAV), found with a frequency of 49%, and six peptides (clones A2 to A7) that differed from RKLRPHWLHFHPVAV by only a few amino acids. Group B contained the second major selected motif (RNVPPIFNDVYRIAF) as well as another homologous peptide (clone B2). Group C represented a 5× selected motif (WKWRHRIPLQLAAGR). In the last group, 18 motifs were selected only once and did not present any similarity with peptides from the other groups. Thus, these motifs were no longer studied. Phages displaying the same motif were pooled, and each motif was tested by ELISA for its immunoreactivity with 6C8D8 (Fig. 1). The highest signal of positivity (absorbance of 2.090) was obtained with the major motif of group A clones (RKLRPHWLHFHPVAV), whereas the

Table 3. Complementarity of mAbs.[a]

	Second alkaline phosphatase-conjugated mAb						
First mAb	6C8D8	5D3D11	12E6H9	5C10D9	7F2F2	5D5A5	11E5C6
6C8D8	−	+	−	−	−	+++	+++
5D3D11	++	−	+	++	++	+++	+++
12E6H9	+	+	−	+	−	+++	+++
5C10D9	++	++	+	−	+	−	+++
7F2F2	+	++	−	+	−	+++	+++
5D5A5	+++	+++	+++	−	+++	−	−
11E5C6	+++	+++	+++	+++	+++	+	−

[a] Enzyme-linked fluorescent assay was performed using VIDAS technology (bioMérieux) with the seven mAbs described in Table 1.

[b] Binding of the second mAb: +++, strong; ++, good; +, weak; −, no binding.

Table 4. Clones isolated by screening the 15merIII phage displayed peptide library with 6C8D8 (anti-f-PSA mAb).

Name of clone	Amino acid sequence	No. of clones
A1	R[a] K L R P H W L H F H P V A V	35 of 72
A2	R K K R R H W I H F H P V A V	1 of 72
A3	R K L R P H R L Y F H P E G V	1 of 72
A4	W K L R P H R L H F H R V A V	1 of 72
A5	R K R R L H R L H Y H R A A G	1 of 72
A6	R K V R P H W I D F H P V A V	1 of 72
A7	R K F R R H N L Y G H P E R E	1 of 72
B1	R N V P P I F N D V Y R I A F	7 of 72
B2	R N V L L I C I D G Y W S A F	1 of 72
C1	W K W R H R I P L Q L A A G R	5 of 72
1–18[b]		18 of 72
Total		72 of 72

[a] Amino acid homologies within group A are underlined.

[b] Clones with no amino acid homologies with groups of clones A, B, or C, and found in only one example.

signal was lower with the seven other group A motifs ($0.955 < \text{absorbance} < 1.770$).

DETERMINATION OF 5D3D11 EPITOPE BY USE OF PHAGE DISPLAYED PEPTIDE LIBRARIES

The mAb 5D3D11 (anti-f-PSA IgG) was used for screening the 15merVIII phage library, using the same approach. After four rounds of biopanning, 36 clones of phages were isolated, their DNA was sequenced, and the motif amino acid sequences were deduced (Table 5). Three motifs (clones 1, 2, and 3) were found in several examples (5, 3, and 2 clones each, respectively). Other motifs were found in only one example and did not display any similarity with the previous motifs. Phages displaying the same motif were pooled, and each different motif was tested by ELISA for its immunoreactivity with 5D3D11 (Fig. 2). The motif that gave the highest signal of positivity was clone 2 (DTPYPWGWLLDEGYD; absorbance, 1.622), although

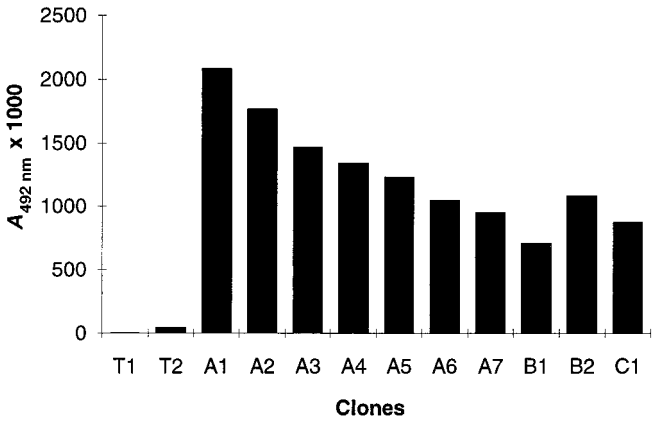

Fig. 1. Immunoreactivity of clones selected with 6C8D8.

Phage clones, described in Table 4, were diluted to the final concentration of 3.2×10^{12} phages/L. The ELISA procedure was performed as described in *Materials and Methods*. Clones *T1* and *T2*, used as negative controls, are phages displaying nonrelevant peptides (DRYLPINGVSMFGVP and TIRSVD) on the pIII protein (15merIII or 6merIII).

Table 5. Clones isolated by screening the 15merVIII phage displayed peptide library with 5D3D11 (anti-f-PSA mAb).

Name of clone	Amino acid sequence	No. of clones
1	R G T Q E W T E L W V S F R A	5 of 36
2	D T P Y P W G W L L D E G Y D	3 of 36
3	M P V S R L C I E L D W C P P	2 of 36
4	W P P P G F N T P P F G S N P	1 of 36
5	S H R H P G V C N S T R P I C	1 of 36
6	Y S F Y A L R G S G R R L V M	1 of 36
7–29[a]		23 of 36
TOTAL		36 of 36

[a] Clones with no amino acid homology with other motifs and found in only one example.

it was selected only three times. Other motifs, including clone 1, the frequency selection of which was higher, were recognized to a lower extent (absorbance <0.647).

RELATIONSHIP BETWEEN RKLRPHWLHFHPVAV AND PSA

The motif RKLRPHWLHFHPVAV (Table 4, clone A1), specifically recognized by 6C8D8, was compared with the PSA sequence. In Western blot experiments performed under reducing conditions (Table 1), 6C8D8 did not bind to PSA, indicating that the 6C8D8 epitope was conformational. As shown in Fig. 3, two regions of this sequence presented some similarities with PSA. The first region (RKLRP, residues 1–5) was similar to either PSA sequence R85–P89 or K145–Q148. The second region (H–FHP, residues 6–12) was similar to the PSA sequence R53–P59. Molecular modeling of the PSA molecule allowed us to visualize the localization of the different PSA homologous regions of RKLRPHWLHFHPVAV, as shown in Fig. 4A. This representation indicates that PSA sequence R53–P59 is joined to PSA sequence K145–Q148, but is distant from the PSA sequence R85–P89. Thus, both the K145–Q148 and R53–P59 sequences could be parts of this conformational epitope. The other selected motifs (Table 4, clones B1, B2, and C) were also compared with the PSA sequence. Motif B1 did not share any homology with PSA. Two amino acid residues of motif B2 (VL) were found in three inaccessible regions of PSA, as well as three amino acid residues of motif C (AGR), which were found to be identical with the inaccessible PSA sequence A175–R177.

RELATIONSHIP BETWEEN DTPYPWGWLLDEGYD AND PSA

The motif DTPYPWGWLLDEGYD (Table 5, clone 2), specifically recognized by 5D3D11, was compared with the PSA sequence. As shown in Fig. 3, only one region of this sequence shared similarity with PSA (PYPWGW, residues 3–8), although this region was similar to three PSA regions (S11–W14, Y129–W133, and S204–G206). However, molecular modeling of the PSA molecule allowed us to distinguish them (Fig. 4B). Indeed, S11–W14 and Y129–W133 were located inside the PSA molecule, and thus would not be accessible to mAb recognition, whereas S204–G206 was located very near the active site.

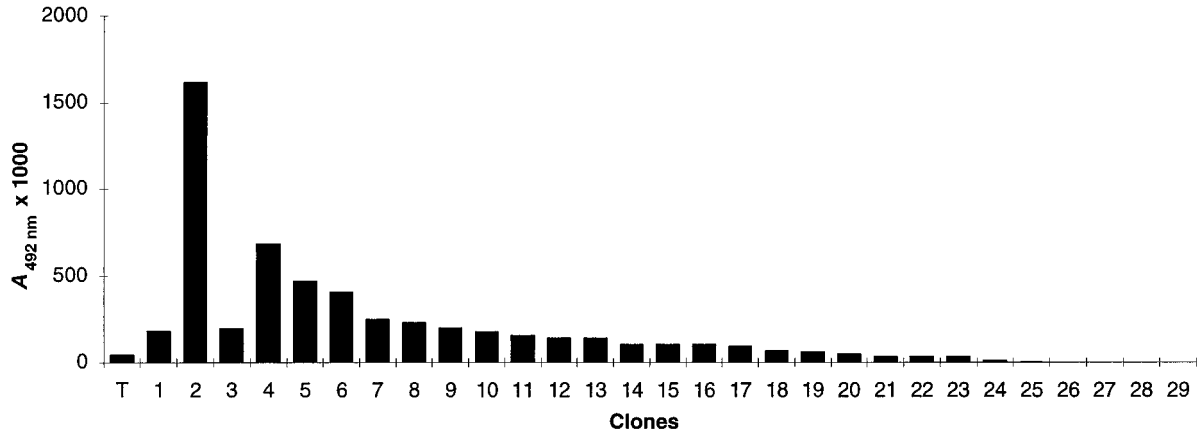

Fig. 2. Immunoreactivity of clones selected with 5D3D11.

Phage clones, described in Table 5, were diluted to the final concentration of 1.6×10^{14} phage/L. The ELISA procedure was performed as described in *Materials and Methods*. Clone *T*, used as negative control, is a phage from the 15VIIImer phage library, displaying a nonrelevant peptide (NACYVDLFLGASVCP).

Moreover, the motif WPPPGFNTPPFGSNP, also selected with mAb 5D3D11 (Table 5, clone 4) and corresponding to the second highest signal of positivity (0.687), contains a four-residue motif homologous to this PSA region (WPPPGFNTPPFGSNP is similar to the S204–E208 PSA sequence).

ASSAYS WITH SYNTHETIC PEPTIDES

The two mimotopes (RKLRPHWLHFHPVAV and DTPYPWGWLLDEGYD) were reproduced as biotinylated synthetic peptides. These biotinylated peptides, coated on the solid phase via streptavidin, were not recognized by their corresponding mAbs (data not shown). On the contrary, the biotinylated peptide bound to the corresponding mAb coated on the solid phase. These results suggested that the presentation of the mimotope was as critical as the presentation of PSA for the antigen-antibody interaction. However, the binding of RKLRPHWLHFHPVAV to 6C8D8, as well as the binding of DTPYP-

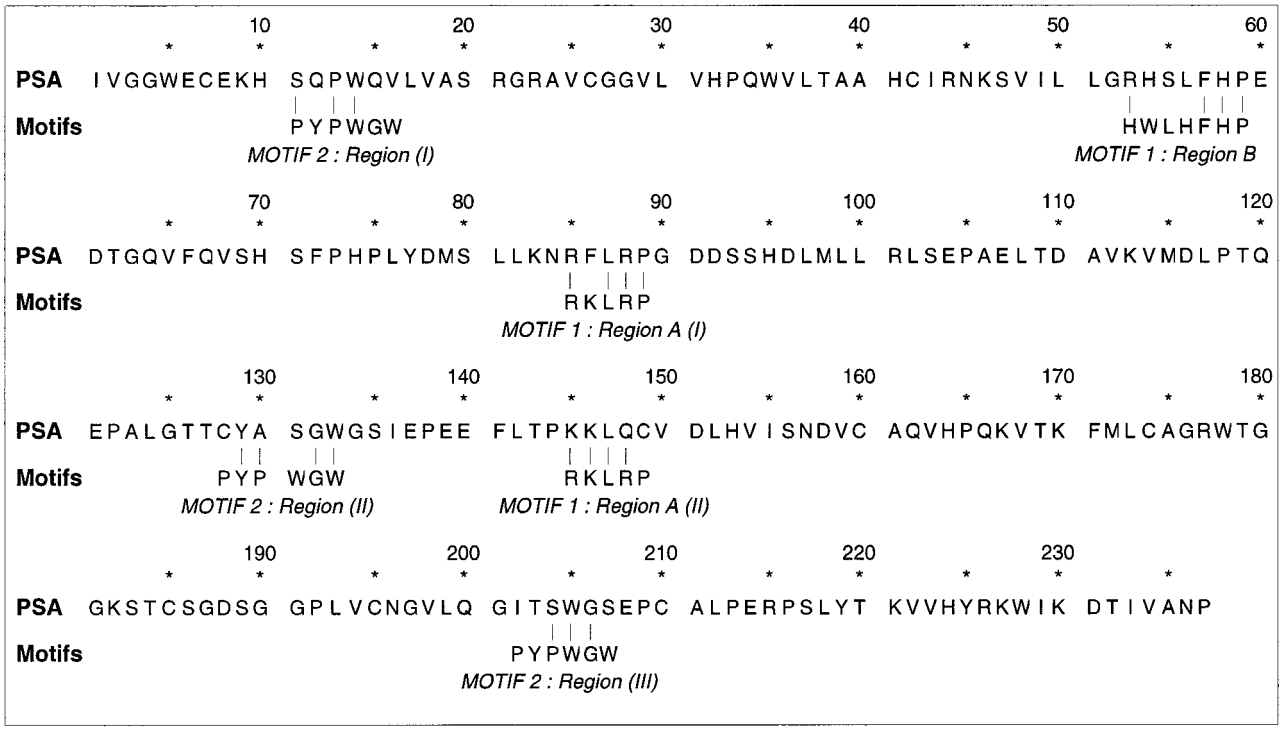

Fig. 3. Amino acid similarity between PSA and selected motifs.

Motif 1 corresponds to RKLRPHWLHFHPVAV, specifically recognized by the anti-f-PSA mAb 6C8D8; *regions A(I)* and *A(II)* correspond to the two possibilities for similarity of RKLRP (residues 1–5 of motif 1) with PSA; *region B* corresponds to the HWLHFHP (residues 6–12 of motif 1) similarity with PSA. *Motif 2* corresponds to DTPYPWGWLLDEGYD, specifically recognized by the anti-f-PSA mAb 5D3D11; *regions (I)*, *(II)*, and *(III)* correspond to the three possibilities for similarity of PYPWGW (residues 3–8 of motif 2) with PSA.

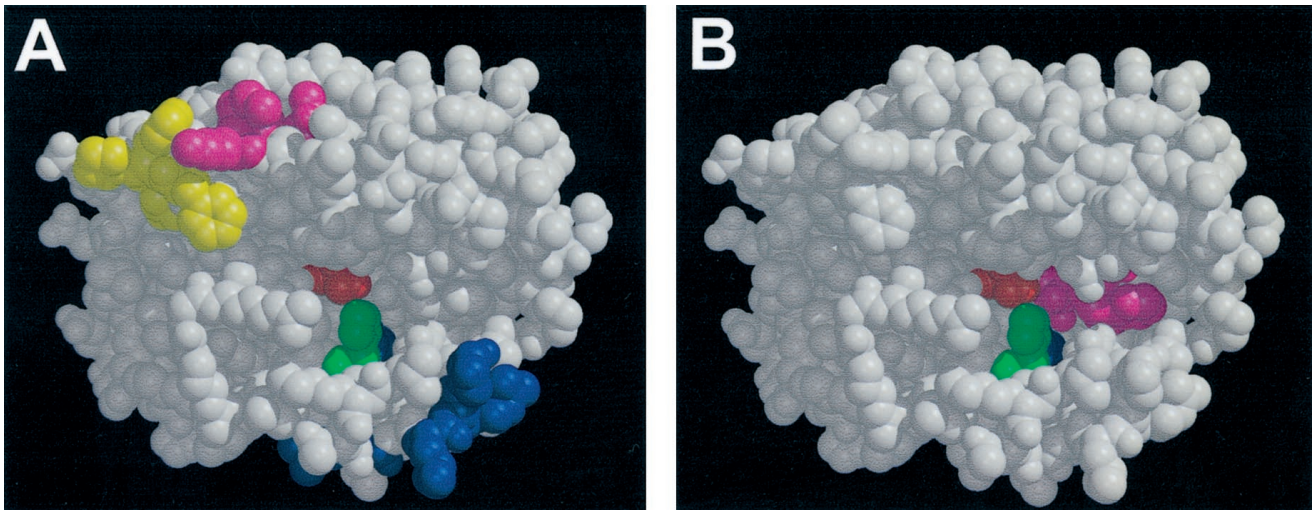

Fig. 4. Molecular modeling of PSA and 6C8D8–5D3D11 epitopes.

PSA appears as a globular protein with a groove containing the active site with the catalytic triad, necessary for the serine protease activity, composed of H41 (*green*), D96 (*blue*), and S189 (*red*). This representation of the PSA molecule allowed us to visualize the localization of the different PSA regions similar to RKLRPHWLHFHPVAV (Fig. 5A) or to DTPYPWGWLLDEGYD (Fig. 5B). (*A*), the PSA sequence R53–E60, similar to region B of RKLRPHWLHFHPVAV (as shown in Fig. 3), is *yellow*. The K145–Q148 PSA sequence, which was the first possibility of similarity with region A of RKLRPHWLHFHPVAV (as shown in Fig. 3), is *pink* and is located near the yellow region defined above. The PSA sequence R85–P89, which was the second possibility of similarity with the region A, is *blue* and is located in the edge of the groove. (*B*), DTPYPWGWLLDEGYD contained one region similar to three PSA regions. S11–W14 and Y129–W133 were located inside the PSA molecule and are not presented, whereas S204–G206 (*pink*) appears to be very near the active site.

WGWLLDEGYD to 5D3D11, could be inhibited by increasing amounts of PSA (Fig. 5).

Inhibition of enzymatic activity by anti-PSA mAbs

The three mAbs specific for f-PSA (6C8D8, 12E6H9, and 5D3D11) and the four anti-t-PSA mAbs (5C10D9, 7F2F2, 5D5A5, and 11E5C6) were tested for their ability to inhibit the enzymatic activity of PSA. As shown in Table 6, when preincubated with PSA, either anti-f-PSA mAb 6C8D8 or 12E6H9 totally inhibited the activity of the enzyme. Under the same conditions, the PSA enzymatic activity was inhibited 53% by 5D3D11. Of the four anti-t-PSA mAbs, 7F2F2 totally inhibited the enzymatic activity of PSA,

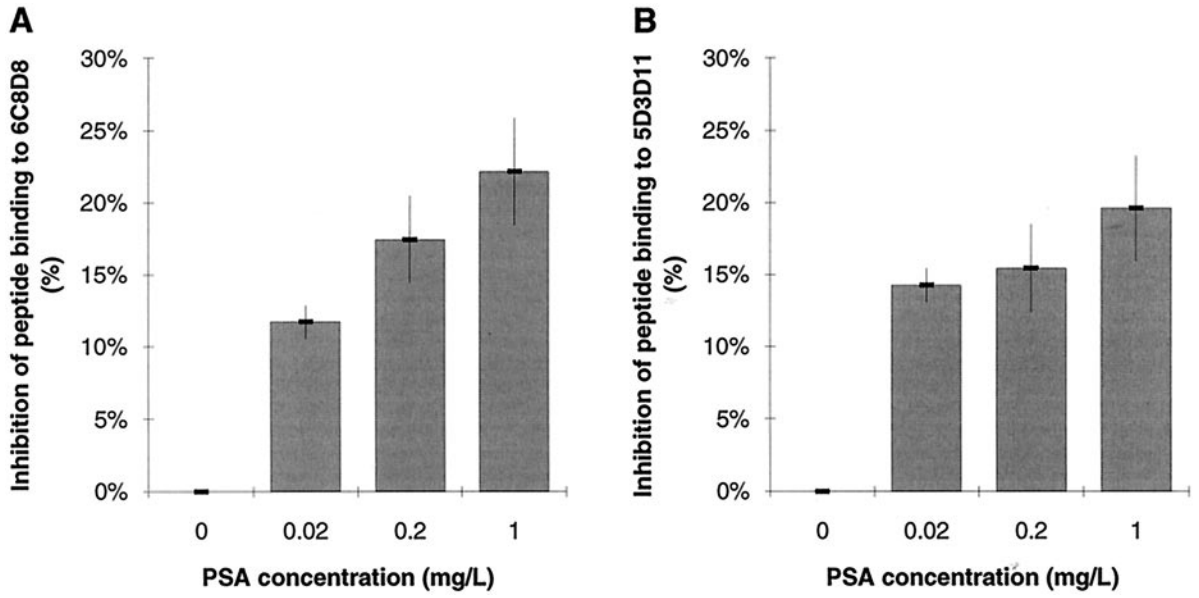

Fig. 5. Assays with synthetic peptides.

(*A*), 6C8D8 was coated on the solid phase. Increasing concentrations of PSA were incubated with the mAb before the addition of 100 mg/L biotinylated peptide RKLRPHWLHFHPVAV. Results are expressed as a percentage of inhibition of the binding of 6C8D8 with RKLRPHWLHFHPVAV by PSA, as indicated in *Materials and Methods*. (*B*), 5D3D11 was coated on the solid phase. Increasing concentrations of PSA were incubated with the mAb before the addition of 100 mg/L biotinylated peptide DTPYPWGWLLDEGYD. Results are expressed as a percentage of inhibition of the binding of 5D3D11 with DTPYPWGWLLDEGYD by PSA, as indicated in *Materials and Methods*.

Table 6. Inhibition of the enzymatic activity of PSA by anti-PSA mAbs.[a]

Anti-PSA mAb	ΔA_{405}/min × 1000	Inhibition, %
PSA alone	26.36 ± 0.16	0.0
Control mAb	26.17 ± 0.46	0.7 ± 2.3
6C8D8	0.24 ± 0.15	99.1 ± 0.6
5D3D11	12.22 ± 0.07	53.6 ± 0.6
12E6H9	0.13 ± 0.08	99.5 ± 0.3
5C10D9	10.50 ± 0.03	60.2 ± 0.4
7F2F2	0.58 ± 0.03	97.8 ± 0.1
5D5A5	11.14 ± 0.02	57.7 ± 0.4
11E5C6	27.26 ± 0.44	−3.4 ± 2.3

[a] PSA was preincubated with either a mAb or buffer as control for 30 min at 37 °C (1 mol PSA/1 mol mAb) before being added to 5 mmol/L substrate S-2586 at a final concentration of 0.4 μmol/L for both PSA and the mAb. The reaction was monitored by measurement of the absorbance at 405 nm for 30 min. PSA preincubated with buffer represented noninhibited PSA activity. PSA was also preincubated with a control mAb, which did bind to PSA, as a control procedure.

whereas 11E5C6 had no significant effect. 5D5A5 and 5C10D9 inhibited the enzymatic activity of PSA 58% and 60%, respectively.

Inhibition of PSA-ACT complex formation by anti-f-PSA mAbs

The three mAbs specific for f-PSA were also tested for their ability to inhibit PSA-ACT complex formation in an ELISA test, using two different anti-t-PSA mAbs (5D5A5 and 11E5C6) coated on the solid phase to display PSA. Although 5D5A5 partially inhibited the enzymatic activity of PSA, whereas 11E5C6 had no significant effect, PSA captured by this mAb could react with ACT (Table 7). However, PSA was unable to complex with ACT when displayed by 5C10D9 and 7F2F2 (data not shown). As shown in Table 7, 6C8D8, 12E6H9, 5C10D9, and 7F2F2 could totally inhibit the complex formation, with PSA displayed by both 5D5A5 and 11E5C6 anti-t-PSA mAbs. Moreover, the percentages of complex formation were low in the presence of 5D3D11 (28% and 34%, respectively). Although 5D5A5 and 11E5C6 should capture different amounts of PSA and affect the ability of PSA to bind ACT, the inhibition of the percentage of relative complex formation by the three anti-f-PSA mAbs was not very different.

Table 7. Inhibition of PSA-ACT complex formation by anti-f-PSA mAbs.[a]

	First mAb (anti-t-PSA)	
Second mAb (anti-f-PSA)	5D5A5 % complex formation	11E5C6 % complex formation
PBS + goat serum	100[b]	100[b]
Control mAb	99.2 ± 3.9[c]	99.7 ± 2.5[c]
6C8D8	0.3 ± 0.5[c]	0.1 ± 1.2[c]
5D3D11	28.0 ± 0.7[c]	34.5 ± 9.2[c]
12E6H9	0.6 ± 0.2[c]	8.6 ± 2.6[c]
5C10D9	NA[d]	0.1 ± 0.7[c]
7F2F2	1.0 ± 0.9[c]	0.0 ± 1.3[c]

[a] ELISA performed as described in *Materials and Methods*, using two different anti-t-PSA mAbs to display PSA (5D5A5 and 11E5C6).

[b] For each anti-t-PSA mAb-captured PSA, the complex formation in the absence of the second mAb corresponds to a relative 100% calibrator calculated as follows: mean absorbance obtained in the presence of ACT − mean absorbance obtained in the absence of ACT.

[c] In the presence of the second mAb, the residual complex formation was determined using the same calculation and expressed as a percentage of the relative 100% calibrator ± 1 SD.

[d] NA, nonapplicable: 5D5A5 and 5C10D9 inhibited themselves, as shown in Tables 2 and 3.

Discussion

Early detection of prostate cancer is critical for adapting treatments against the disease. Thus, the use of f-PSA/t-PSA ratio has been shown to be more reliable for predicting prostate cancer than either transrectal ultrasound or digital rectal examination alone *(42)* and has doubled the proportion of prostate cancers that are confined to the prostate and that are potentially curable at the time of the diagnosis *(4, 43)*.

Currently, most assays use sandwich-type configurations based on the use of two mAbs. Thus, the epitope mapping of generated mAbs appears useful for designing assays that can specifically measure the different forms of PSA. mAbs with specific characteristics (high sensitivity and specificity and equimolar binding to f-PSA and PSA-ACT complex as well as the ability to distinguish between these two immunoreactive forms of PSA) have been reported by several authors *(41, 44–49)*. On the basis of the results of these sandwich assays experiments, several authors have identified different antigenic determinants on the PSA molecule *(44–47)*. By epitope scanning and phage hexapeptide library affinity selection, Jette et al. *(48)* located one conformational epitope near PSA amino acid residues 50–58 among two nonoverlapping epitopes recognized by two anti-t-PSA mAbs. In another study *(49)*, one anti-f-PSA mAb reacted with synthetic peptides corresponding to PSA amino acid residues 50–64 and 55–69, whereas two anti-t-PSA mAbs bound to the peptide 155–175. Recently, using synthetic peptides and computer modeling, Piironen et al. *(41)* restricted the binding specificity of 16 mAbs to four different independent binding regions corresponding to amino acid residues 1–13, 53–64, 80–91, and 151–164, respectively. All anti-f-PSA mAbs tested reacted with the kallikrein loop (residues 84–91), whereas the mAbs binding to other regions were reactive with f-PSA and the PSA-ACT complex as well.

In our study, anti-PSA mAbs could be divided into two groups. The first group included the three anti-f-PSA mAbs 6C8D8, 5D3D11, and 12E6H9, which prevented ACT from binding to PSA. In this group, 6C8D8 and 12E6H9 appeared to bind to a PSA region different from the region bound by 5D3D11. The second group represented the anti-t-PSA mAbs (recognizing both f-PSA and PSA-ACT). Within this group, we were able to distinguish two different categories of mAbs: 5D5A5 and 11E5C6,

which were equimolar and the epitopes of which were far enough from the ACT binding site to allow PSA-ACT complex formation when one of these mAbs was bound to PSA; and 5C10D9 and 7F2F2, which preferentially bound to f-PSA and were able to inhibit PSA-ACT formation. Such results suggest that the inhibition of PSA-ACT complex formation could occur either by steric hindrance or by PSA conformation change induced by the binding of the anti-t-PSA mAb.

When tested by pairs in sandwich assays and competition experiments, many mAb couples appeared to be independent: no inhibition was observed whatever the order of addition of the respective mAbs (mAb1 + mAb2 or mAb2 + mAb1). Thus, their respective epitopes should be distant on the PSA molecule (the three anti-f-PSA mAbs vs 5D5A5 and 11E5C6). On the other hand, a significant competition between some mAbs was observed whatever the order of mAb addition (12E6H9/6C8D8, or 11E5C6/5D5A5). This suggests that both mAbs could recognize epitopes on the PSA molecule that are not distant, but it is more likely that these mAbs inhibit themselves by steric hindrance. The slight discrepancies observed between results obtained in competition experiments or in sandwich assays might be attributable to differences in the presentation of PSA, either displayed by the first mAb (sandwich assays) or coated on ELISA plate wells (competition experiments). Indeed, in competition experiments, the inhibition rates often depended on the addition order of the mAbs (6C8D8/7F2F2, or 5C10D9/5D5A5), suggesting that the inhibition could be because of conformational changes induced by the binding of the first mAb. The particular effects of 5D3D11, 5D5A5, and 11E5C6 to enhance the ability of other mAbs to bind to PSA could be in agreement with such a hypothesis.

Localizing the binding sites of mAbs on their protein antigen makes them much more useful reagents. Thus, the phage library technology has become a powerful tool for epitope mapping of antibodies *(30, 50–52)*. The selected peptides, so-called mimotopes, mimic the binding characteristics of the natural epitope. However, different data suggest that if the epitope is continuous, the homology between phage epitope sequences and the antigen sequence may be high, whereas in the case of noncontinuous epitopes, there may be little or no homology at all with the antigen sequence *(53)*.

The screening of the 15merIII phage displayed peptide library with the anti-f-PSA mAb 6C8D8 mainly selected the mimotope RKLRPHWLHFHPVAV. Two short sequences of RKLRPHWLHFHPVAV were similar to two different PSA regions, distant in the primary sequence (R53–P59 and K145–Q148) but adjacent in the tertiary structure, that could be part of a conformational epitope. The residues RKLRP as well as the residues FHP were highly conserved in the group A selected phage clones: residue K2, which is identical to PSA residue K146, and residue H11, which is identical to PSA residue H58, were completely conserved, whereas some others residues, which are not similar to PSA, could be replaced by close residues (W7 replaced by R or L8 replaced by I). This is in agreement with the respective importance of each epitope amino acid, as reported previously *(54, 55)*. Moreover, this region was contained in the ACT binding site, around the PSA active site, as described by Villoutreix et al. *(56)*. This finding was connected with the hypothesis that specific anti-f-PSA epitopes are masked when ACT binds to PSA *(7)* and that 6C8D8 could totally inhibit PSA-ACT complex formation. In the same way, 12E6H9, which recognized a close but different epitope from the 6C8D8 epitope, could totally inhibit PSA enzymatic activity by preventing the substrate from entering the groove and being hydrolyzed at the active site.

PSA region R53–P59 has been reported to be an epitope presented on PSA-ACT *(41, 48)*. However, in another study *(49)*, it was reported as a region bound by an anti-f-PSA mAb, which is in agreement with our results. The fact that this region could be described either as an anti-t-PSA mAb epitope or as an anti-f-PSA mAb epitope could explain why the binding of 6C8D8 (anti-f-PSA mAb) with PSA could be inhibited by 7F2F2 (anti-t-PSA mAb).

The three other selected motifs (Table 4, B1, B2, and C), also recognized by 6C8D8, did not allow us to localize the epitope because they did not share any significant homology with PSA. Thus, these motifs could only mimic the epitope conformation, as reported previously *(53)*.

According to the Western blot experiments and sandwich assays, the anti-f-PSA mAb 5D3D11 epitope was also conformational and bound to another PSA region. Perhaps because of the weak affinity of 5D3D11 for PSA, none of the different motifs obtained by phage library screening was selected with high frequency. Nevertheless, ELISAs of the phage clones allowed us to select mimotopes specifically recognized by this mAb. Moreover, when reproduced as a synthetic biotinylated peptide, one of the selected mimotopes (DTPYPWGWLLDEGYD) was able to affect the binding of PSA to 5D3D11. On the basis of amino acid similarities and molecular modeling, two mimotopes (DTPYPWGWLLDEGYD and WPPPGFNTPPFGSNP) appeared to mimic a conformational epitope, one part of which was located in a proximal region of the enzymatic site: the residue W205 was on the board of the groove containing the active site, whereas the residue S204 was located inside the groove. This region was also not very accessible because of the groove, and this finding could explain the weak affinity of this mAb for PSA. Furthermore, the close proximity of the epitope to the PSA active site correlated with the specificity of 5D3D11 for f-PSA. However, the mAb inhibited complex formation 65–72%, depending on the ability of the anti-t-PSA mAb coated on the ELISA solid phase to display PSA. The weak affinity of 5D3D11 for PSA could lead to a balance shift in favor of ACT and then to an incomplete inhibition of formation of the complex. ACT was unable to complex with PSA coated directly on the ELISA solid phase (data

not shown), suggesting that the anti-t-PSA mAb coated on the ELISA solid phase imposed a certain conformation on the displayed PSA. This constraint determined the ability of ACT to compete with 5D3D11. The weak 5D3D11 affinity could also explain the partial inhibition of the PSA enzymatic activity (53%) observed in soluble and equimolar ratio conditions.

The specificity of each mimotope was supported by the ability of its corresponding biotinylated synthetic peptide to be captured by the respective mAb. Moreover, this capture was inhibited by increasing amounts of PSA.

The mimotopes selected with the two anti-f-PSA mAbs mimicked two different epitopes on the PSA molecule. For both, at least one part of each epitope was located in the ACT binding site. The binding of these two anti-f-PSA mAbs to PSA inhibited PSA-ACT formation. However, we cannot emphasize that the inhibition of complex formation is a characteristic of anti-f-PSA mAbs. As reported previously *(47)*, an anti-t-PSA mAb bound to PSA could prevent ACT from binding to PSA by steric hindrance or conformational changes. In our study, the 5C10D9 and 7F2F2 epitopes were probably located at the edge of the ACT binding site. This location allowed the respective mAbs to recognize the PSA-ACT complex.

In conclusion, this epitope determination could be a starting point to better anti-f-PSA selection. Taking into account all biochemical, immunological, and molecular data, this study has determined two different regions on the PSA molecule that were recognized by anti-f-PSA mAbs. Moreover, our results demonstrate that the conformation of these regions is critical for antibody recognition. Thus, this study, together with others *(41, 44–49)*, helps in the understanding of the immunological activities of PSA, which could be useful for generation of new clinically relevant assays for this antigen.

References

1. Lundwall A, Lilja H. Molecular cloning of human prostate specific antigen cDNA. FEBS Lett 1987;214:317–22.
2. McCormack RT, Rittenhouse HG, Finlay JA, Sokoloff RL, Wang TJ, Wolfert RL, et al. Molecular forms of prostate-specific antigen and the human kallikrein gene family: a new era. Urology 1995;45: 729–44.
3. Sensabaugh GF. Isolation and characterization of a semen-specific protein from human seminal plasma: a potential new marker for semen identification. J Forensic Sci 1978;23:106–15.
4. Catalona WJ, Smith DS, Ratliff TL, Dodds KM, Coplen DE, Yuan JJ, et al. Measurement of prostate specific antigen in serum as a screening test for prostate cancer. N Engl J Med 1991;324: 1156–61.
5. Stamey TA, Yang N, Hay AR, McNeal JE, Freiha FS, Redwine E. Prostate specific antigen as a serum marker for adenocarcinoma of the prostate. N Engl J Med 1987;317:909–16.
6. Christensson A, Laurell CB, Lilja H. Enzymatic activity of prostate-specific antigen and its reactions with extracellular serine proteinase inhibitors. Eur J Biochem 1990;194:755–63.
7. Lilja H, Christensson A, Dahlén U, Matikainen MT, Nilsson O, Pettersson K, Lövgren T. Prostate-specific antigen in serum occurs predominantly in complex with alpha-1-antichymotrypsin. Clin Chem 1991;37:1618–25.
8. Espana F, Sanchez-Cuenca J, Estelles A, Gilabert J, Griffin JH, Heeb MJ. Quantitative immunoassay for complexes of prostate specific antigen with α_2-macroglobulin. Clin Chem 1996;42:545–50.
9. Stenman UH, Leinonen J, Alfthan H, Rannikko S, Tuhkanen K, Alfthan O. A complex between prostate specific antigen and α-1 antichymotrypsin is the major form of prostate specific antigen in serum of patients with prostatic cancer: assay of the complex improves clinical sensitivity for cancer. Cancer Res 1991;51: 222–6.
10. Christensson A, Bjork T, Nilsson O, Dahlén U, Matikainen MT, Cockett ATK, et al. Serum prostate specific antigen complexed to α_1-antichymotrypsin as an indicator of prostate cancer. J Urol 1993;150:100–5.
11. Bangma CH, Kranse R, Blijenberg PG, Schroder FH. The free-to-total serum prostate specific antigen ratio for staging prostate carcinoma. J Urol 1997;157:544–7.
12. Elgamal AAA, Cornillie FJ, Van Poppel HP, Van devoorde WM, Mccabe R, Baert LV. Free-to-total prostate specific antigen ratio as a single test for detection of significant stage T1c prostate cancer. J Urol 1996;156:1042–7.
13. Toubert ME, Guillet J, Chiron M, Meria P, Role C, Schlageter MH, et al. Percentage of free serum prostate specific antigen: a new tool in the early diagnosis of prostatic cancer. Eur J Cancer 1996;32A:2088–93.
14. Vancangh PJ, Denayer P, Sauvage P, Tombal B, Elsen M, Lorge F, et al. Free to total prostate-specific antigen (PSA) ratio is superior to total-PSA in differentiating benign prostate hypertrophy from prostate cancer. Prostate Suppl 1996;7:30–4.
15. Zhou AM, Tewari PC, Bluestein BI, Caldwell GW, Larson FI. Multiple forms of prostate specific antigen in serum: differences in immunorecognition by monoclonal and polyclonal assays. Clin Chem 1993;39:2483–91.
16. Lundwall A. Characterization of the gene for prostate specific antigen, a human glandular kallikrein. Biochem Biophys Res Commun 1989;162:451–9.
17. Villoutreix BO, Getzoff ED, Griffin JH. A structural model for the prostate disease marker, human prostate specific antigen. Protein Sci 1994;3:2033–4.
18. Köhler G, Milstein C. Continuous culture of fused cells secreting antibody of predefined specificity. Nature 1975;256:495–7.
19. Köhler G, Milstein C. Derivation of specific antibody producing tissue, culture and tumor lines by cells fusion. Eur J Immunol 1976;6:511–9.
20. Gretch DR, Suter M, Stinski MF. The use of biotinylated monoclonal antibodies and streptavidin affinity chromatography to isolate herpes virus hydrophobic proteins or glycoproteins. Anal Biochem 1987;163:270–7.
21. Laemmli UK. Cleavage of structural proteins during the assembly of the head of bacteriophage T4. Nature 1970;227:680–5.
22. Towbin H, Staehelin T, Gordon J. Electrophoretic transfer of proteins from polyacrylamide gels to nitrocellulose sheets: procedure and some applications. Proc Natl Acad Sci U S A 1979;76: 4350–4.
23. Zeder-Lutz G, Zuber E, Witz J, Van Regenmortel MHV. Thermodynamic analysis of antigen-antibody binding using biosensor measurements at different temperatures. Anal Biochem 1997;246: 123–32.
24. Oddie GW, Gruen LC, Odgers GA, King LG, Kortt AA. Identification and minimization of nonideal binding effects in BIAcore analysis: ferritin/anti-ferritin Fab′ interaction as a model. Anal Biochem 1997;244:301–11.
25. Löfas S, Johnsson B. A novel hydrogel matrix on gold surfaces in

plasmon resonance sensors for fast and efficient covalent immobilization of ligands. J Chem Soc Chem Commun 1990;21: 1526–8.
26. Pellequer JL, Van Regenmortel MHV. Measurement of kinetic constants of viral antibodies using a new biosensor technology. J Immunol Methods 1993;166:133–43.
27. Weber B, Doerr HW. Evaluation of the automated VIDAS system for the detection of anti-HIV-1 and anti-HIV-2 antibodies. J Virol Methods 1993;42:63–74.
28. Mikkelsen AL, Borggaard B, Lebech PE. Results of serial measurement of estradiol in serum with six different methods during ovarian stimulation. Gynecol Obstet Investig 1996;41:35–40.
29. Pittet JL, Barbalat V, Sanvert M, Villard C, Jorieux S, Mazurier C. Evaluation of a new automated ELISA test for von Willebrand factor using two monoclonal antibodies. Blood Coagul Fibrinolysis 1997;8:209–15.
30. Scott JK, Smith GP. Searching for peptide ligands with an epitope library. Science 1990;249:386–90.
31. Smith GP, Scott JK. Libraries of peptides and proteins displayed on filamentous phage. Methods Enzymol 1993;217:228–57.
32. Dybwad A, Forre O, Natvig J, Sioud M. Structural characterizations of peptides that bind synovial fluid antibodies from RA: a novel strategy for identification of disease-related epitopes using a random peptide library. Clin Immunol Immunopathol 1995;75:45–50.
33. Sambrook J, Fritsch EF, Maniatis T, eds. Molecular cloning. a laboratory manual. Cold Spring Harbor, NY: Cold Spring Harbor Laboratory Press, 1982.
34. Sanger F, Nicklen S, Coulson AR. DNA sequencing with chain-terminating inhibitors. Proc Natl Acad Sci U S A 1977;74:5463–7.
35. Pearson WR, Lipman DJ. Improved tools for biological sequence analysis. Proc Natl Acad Sci U S A 1988;85:2444–8.
36. Watt KWK, Lee PJ, M'Timkulu T, Chan WP, Loor R. Human prostate specific antigen: structural and functional similarity with serine proteases. Proc Natl Acad Sci U S A 1986;83:3166–70.
37. Schaller J, Akiyama K, Tsuda R, Hara M, Marti T, Rickli E. Isolation, characterization and amino-acid sequence of gamma-seminoprotein, a glycoprotein from human seminal plasma. Eur J Biochem 1987;170:111–20.
38. Sayle R, Milner-White EJ. RASMOL: biomolecular graphics for all. Trends Biochem Sci 1995;20:374.
39. Jolivet-Reynaud C, Dalbon P, Viola F, Yvon S, Paranhos-Baccala G, Piga N, et al. HCV core immunodominant region analysis using mouse monoclonal antibodies and human sera: characterization of major epitopes useful for antigen detection. J Med Virol 1998;56:342–50.
40. Deibel MR, Lobl TJ, Yem AW. A technique for rapid purification of low yield products: biotinylation of chemically synthesized proteins on-resin. Peptide Res 1989;2:189–94.
41. Piironen T, Villoutreix BO, Becker C, Hollingsworth K, Vihinen M, Bridon D, et al. Determination and analysis of antigenic epitopes of prostate specific antigen (PSA) and human glandular kallikrein 2 (hK2) using synthetic peptides and computer modeling. Protein Sci 1998;7:259–69.
42. Cooner WH, Mosley BR, Rutherford CL Jr, Beard JH, Pond HS, Terry WJ, et al. Prostate cancer detection in clinical urological practice by ultrasonography, digital rectal examination and prostate specific antigen. J Urol 1990;143:1146–54.
43. Catalona WJ, Richie JP, Ahmann FR, Hudson MA, Scardino PT, Flanigan RC, et al. Comparison of digital rectal examination and serum prostate specific antigen in the early detection of prostate cancer: results of a multicenter clinical trial of 6,630 men. J Urol 1994;151:1283–90.
44. Frankel AE, Rouse RV, Wang MC, Chu TM, Herzenberg LA. Monoclonal antibodies to a human prostate antigen. Cancer Res 1982;42:3714–8.
45. Pettersson K, Piironen T, Seppälä M, Liukkonen L, Christensson A, Matikainen MT, et al. Free and complexed prostate specific antigen (PSA): in vitro stability, epitope map, and development of immunofluorometric assays for specific and sensitive detection of free PSA and PSA α_1-antichymotrypsin complex. Clin Chem 1995; 41:1480–8.
46. Nilsson O, Peter A, Andersson I, Nilsson K, Grundström B, Karlsson B. Antigenic determinants of prostate specific antigen (PSA) and development of assays specific for different forms of PSA. Br J Cancer 1997;75:789–97.
47. Corey E, Wegner SK, Stray JE, Corey MJ, Arfman EW, Lange PH, Vessella RL. Characterization of 10 new monoclonal antibodies against prostate specific antigen by analysis of affinity, specificity and function in sandwich assays. Int J Cancer 1997;71:1019–28.
48. Jette DC, Kreutz FT, Malcolm BA, Wishart DS, Noujaim AA, Suresh MR. Epitope mapping of prostate-specific antigen with monoclonal antibodies. Clin Chem 1996;42:1961–9.
49. Corey E, Wegner SK, Corey MJ, Vessella RL. Prostate-specific antigen: characterization of epitopes by synthetic peptide mapping and inhibition studies. Clin Chem 1997;43:575–84.
50. Cwirla SE, Peters EA, Barret RW, Dower WJ. Peptides on phage: a vast library of peptides for identifying ligands. Proc Natl Acad Sci U S A 1990;87:6378–82.
51. Devlin JJ, Panganiban LC, Delvin PE. Random peptide libraries: a source of specific protein binding molecules. Science 1990;249: 404–6.
52. Zhong G, Smith GP, Berry J, Brunham RC. Conformational mimicry of a chlamydial neutralization epitope on filamentous phage. J Biol Chem 1994;269:24183–8.
53. Yayon A, Aviezer D, Safran M, Gross JL, Heldman Y, Cabilly S, et al. Isolation of peptides that inhibit binding of basic fibroblast growth factor to its receptor from a random phage-epitope library. Proc Natl Acad Sci U S A 1993;90:10643–7.
54. McKean PG, O'Dea K, Brown KN. A single amino acid determines the specificity of a monoclonal antibody which inhibits *Plasmodium chabaudi* AS in vivo. Mol Biochem Parasitol 1993;62:211–22.
55. Ludmerer SW, Benincasa D, Mark GE III. Two amino acid residues confer type specificity to a neutralizing, conformationally dependent epitope on human papillomavirus type 11. J Virol 1996;70: 4791–4.
56. Villoutreix BO, Lilja H, Pettersson K, Lövgren T, Teleman O. Structural investigation of the α-1-antichymotrypsin: prostate specific antigen complex by comparative model building. Protein Sci 1996;5:836–51.